Mechanism and Kinetics Parameters of the Reduction Reaction of NO by CO on Pd/Al_2O_3 Catalyst

Joaquín Cortés,* Eliana Valencia, Jorge Herrera, and Paulo Araya

Facultad de Ciencias Físicas y Matemáticas, Universidad de Chile, Casilla 2777, Santiago, Chile

By means of a mechanism similar to that used by Peden and Permana for the reduction reaction of NO by CO on Rh and the analytical solution of its kinetics equations, a set of kinetics parameters that interpret some experimental results determined at moderate pressures for that reaction on palladium supported on alumina were established. When using those parameters, the kinetics model, studied through the analytic solution of the kinetics equations and Monte Carlo simulations, presents various aspects of interest such as the maximum found in experiments in the literature for production versus CO concentration or temperature and a change in the sign of reaction order with respect to CO and NO between the high- and low-temperature zones, and it shows the characteristic configurations of the adsorbed phase in the square and hexagonal cases. Monte Carlo simulations at high temperatures on a square lattice show a behavior similar to that of the classical model of Brosilow−Ziff, with a phase poisoned with pairs of superficial nitrogens in a diagonal direction.

Introduction

The catalytic reduction reaction of NO by CO (CO−NO reaction) over a variety of noble and transition metals has been, together with the oxidation reaction of CO, one of the most widely studied surface reactions over the last decades. This is due, particularly, to its importance in the catalytic elimination of nitrogen oxides (NO_x), produced mainly in the exhaust gases of automobiles and leading to serious pollution problems, with the introduction in the late 1970s of the three-way catalytic converter.[1] These reactions have also been interesting examples for the theoretical study of irreversible dynamics systems that have complicated behaviors such as oscillations, kinetics phase transitions, and other interesting phenomena.[2] These aspects have also been reviewed recently by Evans,[3] Zhdanov,[4] and Albano.[5]

Rhodium and platinum have been the most widely studied metals because of their excellent catalytic behavior, and for that reason, they have been used preferentially in automobile converters. During the past few years, however, there has been increasing interest in the use of palladium, not only because of its lower cost due to its greater abundance but also because, in addition to having a good behavior in the oxidation of hydrocarbons, it has greater resistance to being sinterized at high temperatures.[6−8] Improvements in the purification of gasoline, on the other hand, have decreased the problem of the lower resistance shown by Pd, compared to the other noble metals, to poisoning with S and Pb.

The delay in research with Pd catalysts with respect to those of Rh and Pt has meant a greater uncertainty about the microscopic behavior reflected in the kinetics mechanism, in the case of the CO−NO reaction on Pd, as mentioned recently.[6,8] However, the closeness of the three metals mentioned so far in the periodic table of the elements may hint that the mechanism should not be too different for all of them. This explains why there have been recent attempts to associate the mechanism on Pd with the previously known mechanisms on Rh for the same reaction.[6−8] Information on the experimental kinetics is also still scarce and conflicting, almost certainly because different experimental techniques and conditions have been used. Reiner et al.,[9,10] for example, published data obtained with a conventional flow reactor, while G. Prevot,[6] Nakao et al.,[7] and K. Thirumoorthy[8] used molecular beam techniques. This means that no reliable information is available on kinetics parameters such as activation energy and frequency factors of the elemental reactions involved at moderately high pressures, despite recent interesting contributions in that respect that have been published[6,7] for the low-pressure region.

The mechanism on Rh has a long and conflicting history since the early work of Hecker and Bell,[11] followed by, among others, the work of Oh,[12] Cho,[13] Chuang and Tan,[14] Peden[15] and Permana,[16] and that from our laboratory,[17,18] where we have considered recent experiments of Zaera's group.[19] In view of the attractive matters discussed previously with respect to this mechanism, included also in a large number of theoretical papers, with some contributions from our laboratory,[20] it seems appropriate to make use of the recent interest in Pd as a catalyst to extend those studies. This will allow a better understanding of the microscopic behavior of this interesting reaction whose possible applications have stimulated current interest.

In view of the above considerations, in this paper, we will examine the behavior of the kinetics mechanism and its parameters in the CO−NO reaction on Pd under moderate pressure, assuming elemental stages similar to those proposed previously for Rh. With that purpose, we have carried out some laboratory experiments with a sample of Pd supported on alumina, complementing them with an analysis by means of kinetics equations and Monte Carlo simulations.

Experimental Procedure

A 1% Pd/Al_2O_3 catalyst was prepared by impregnating γ-Al_2O_3 (BAFF) with an appropriate amount of an aqueous solution of $Pd(NO_3)_2$ (Merck). The impregnated support was

* To whom correspondence should be addressed. E-mail: jcortes@dqb.uchile.cl.

then dried in an oven at 105 °C for 12 h. The dispersion, determined by the chemisorption of hydrogen, was equal to 23.4%.

To determine the catalytic activity, 0.2 grams of catalyst was loaded into a 50 cm long and 1 cm diameter tubular reactor. The catalyst was calcined in situ for 1 h at 500 °C in a 10 cm^3/min stream of pure O_2, cooled to 300 °C, and reduced in a flow of 30 cm^3/min of a 5% H_2/Ar stream for 1 h. After that, the feed was switched to pure He and maintained at 300 °C for 1 h. The reactor temperature was then decreased to room temperature, and the reactants were allowed to flow (90 cm^3/min) at a concentration of 2.7% CO and 5.2% NO, the balance being He, corresponding to 20.52 Torr of CO and 39.52 Torr of NO. The temperature was increased at a ramp rate of 2 °C/min using an RKC model REX-P100 programmer, taking data at the temperatures used in the paper. The reactor inlet and outlet streams were analyzed by gas chromatography using two PerkinElmer Autosystem chromatographs equipped with HWD detectors. The first chromatograph had a HAYASEP D (2 m × 1/8 in.) column to analyze CO_2 and N_2O, and the second had an MS 5A (1 m × 1/8 in.) column to analyze CO. The conversion of NO and CO was calculated from the C and N mass balance, considering that the only nitrogen-containing products were N_2 and N_2O and the only carbon-containing product was CO_2, according to the following reaction pathways

$$CO + 2NO = CO_2 + N_2O \quad (1)$$

$$CO + NO = CO_2 + \frac{1}{2}N_2 \quad (2)$$

Therefore, the N_2 concentration ($[N_2]$) was estimated from the equation

$$[N_2] = \frac{1}{2}([CO_2]_t - [N_2O]) \quad (3)$$

where $[CO_2]_t$ and $[N_2O]$ are the CO_2 and N_2O concentrations, respectively, in the reactor effluent.

The Reaction Mechanism and the Kinetics Parameters. With the purpose of getting a set of kinetics parameters in the zone of moderately high pressures, ramp experiments were carried out, increasing the temperature at 2 °C/min, for the CO−NO reaction on a 1% Pd/Al_2O_3 catalyst, as described in the previous section. Figure 1 shows the experimental results of CO_2 production and the selectivity of nitrogen at certain temperatures. The graph also includes theoretical curves obtained from the kinetics equations of the mechanism given in Scheme 1 with the kinetics parameters of Table 1, which will be analyzed below.

As has been mentioned,[6,8] the microscopic behavior of the kinetics of the CO−NO reaction on Pd is not fully understood. However, because of the closeness in the periodic table, a reaction mechanism similar to that of Langmuir Hinshelwood (LH), used by Peden[15] and Permana[16] for the same reaction on Rh, has recently been proposed by various authors as probable. This mechanism, whose elemental stages appear in Scheme 1, has been used in this paper.

As far as the authors have reviewed, only in two recent articles are there are proposals for a set of kinetics parameter values for the reaction in question on Pd.[6,7] Those data have been determined experimentally using a molecular beam reaction system in low-pressure and UHV zones, showing only the appearance of CO_2 and N_2 as products. For that reason, both cases considered a mechanism like that of Scheme 1 that excludes step 8, the formation of N_2O.

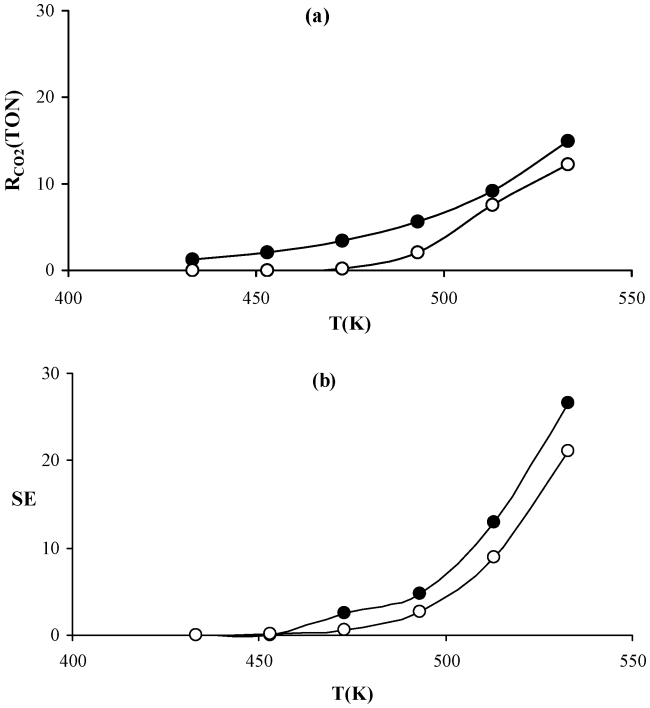

Figure 1. (a) CO_2 production, R_{CO_2}, as a function of temperature T. (b) Selectivity, SE, versus temperature, T; experimental data (●), theoretical MFT data (○). The lines have been drawn to guide the eyes; $p_{CO} = 20.52$ and $p_{NO} = 39.52$ Torr.

SCHEME 1: Mechanism of the CO−NO Reaction Used in the Paper

$$CO + S \underset{k_1}{\longleftrightarrow} CO_{(a)} \quad (1)$$

$$CO_{(a)} \xrightarrow{k_2} CO + S \quad (2)$$

$$NO + S \xrightarrow{k_3} NO_{(a)} \quad (3)$$

$$NO_{(a)} \xrightarrow{k_4} NO_{(a)} + S \quad (4)$$

$$NO(a) + S \xrightarrow{k_5} N(a) + O(a) \quad (5)$$

$$2N_{(a)} \xrightarrow{k_6} N_2 + 2S \quad (6)$$

$$CO_{(a)} + O_{(a)} \xrightarrow{k_7} CO_2 + 2S \quad (7)$$

$$NO(a) + N(a) \xrightarrow{k_8} N_2O + 2S \quad (8)$$

TABLE 1: Kinetics Parameters of K. Nakao et al.[7] and the Fitting Parameters Used in the Paper

event	activation energy E_i (kcal/mol)	frequency factor ν_i (sec^{-1})
CO desorption (k_2)	35.5	1.0×10^{17}
NO desorption (k_4)	36.0	1.0×10^{17} (1.0×10^{18})[a]
NO dissociation (k_5)	34.2	2.7×10^{14} (7.9×10^{21})[a]
N_2 production (k_6)	29.0	6.5×10^{13}
N_2O production (k_8)	32.7[b]	5.3×10^{13}[b] (5.3×10^{16})[a]
CO_2 production (k_7)	33.6	7.1×10^{15} (1.2×10^{16})[a]

[a] Values of ν_i in parentheses correspond to a fit with experimental data from Figure 1. [b] Parameters of ref 17.

Table 1 shows the kinetics parameters of the various steps of the mechanism obtained in 2005 by K. Nakao et al.,[7] together with the values for step 8 proposed previously for Rh[17] because no information is available for that step in the case of Pd. On the basis of that information, an interpretation was made of the

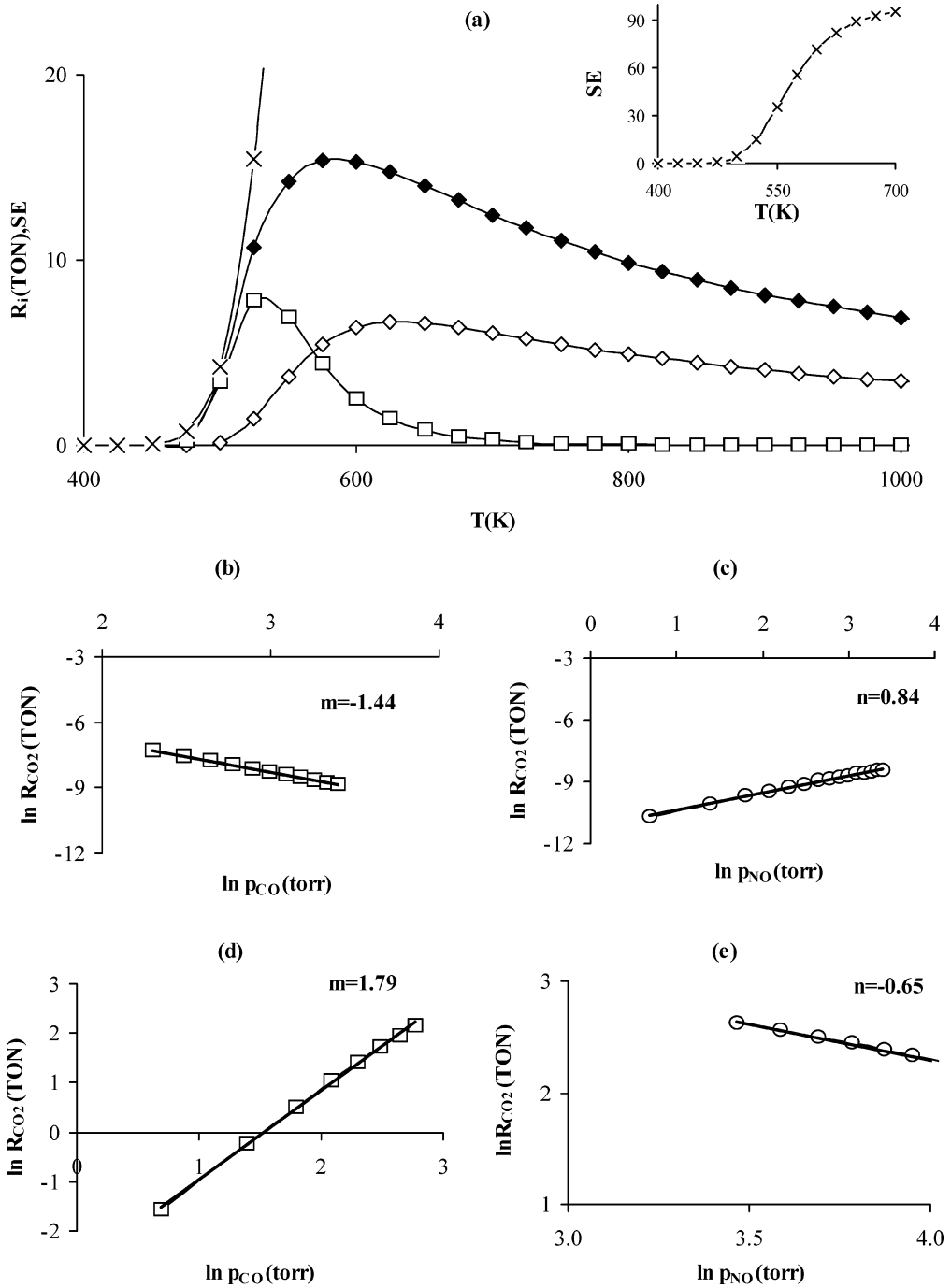

Figure 2. (a) R_i productions as a function of temperature T. (b) CO_2 production as a function of CO pressure with a fixed NO pressure of 39.52 Torr at 433 K in the steady state for the constants of Table 1 and the MFT model. (c) The same as (b) as a function of NO pressure with a fixed CO pressure of 20.52 Torr. (d) The same as (b) at 533 K. (e) The same as (c) at 533 T. (◆) R_{CO_2}; (◇) R_{N_2}; (□) R_{N_2O}; (X) SE.

experimental data of Figure 1. For that purpose, use was made of the analytical expressions of the mean field kinetic model corresponding to the mechanism of Scheme 1, whose details and assumptions are detailed in Appendix A. Application of the parameters of K. Nakao et al., corresponding to crystal face (110), gave productions close to zero for the pressure and temperature of the paper. For that reason, in the case of the supported catalysts of our experiment, the values of the kinetics constants of NO desorption and dissociation and of CO_2 and N_2O production were fitted. The results obtained are shown in parentheses in Table 1. The difficulty in interpreting kinetics information in the moderate- and high-pressure zones with data obtained in the zone of low pressure has been called the pressure-gap problem.[11] This matter has been discussed in detail by Zhdanov[12] in the case of the CO−NO reaction on Rh, with rather discouraging results.

Results and Discussion

The theoretical curves of Figure 1 were calculated with the fitting parameters of Table 1 and the mean field theoretical model. The fit obtained is reasonable if it is considered that the objective of getting unique parameters valid over a wide temperature range is always difficult. For example, G. Prevot et al.,[6] who got a less satisfactory fit than ours for this system within a similar temperature range, point out that it is not

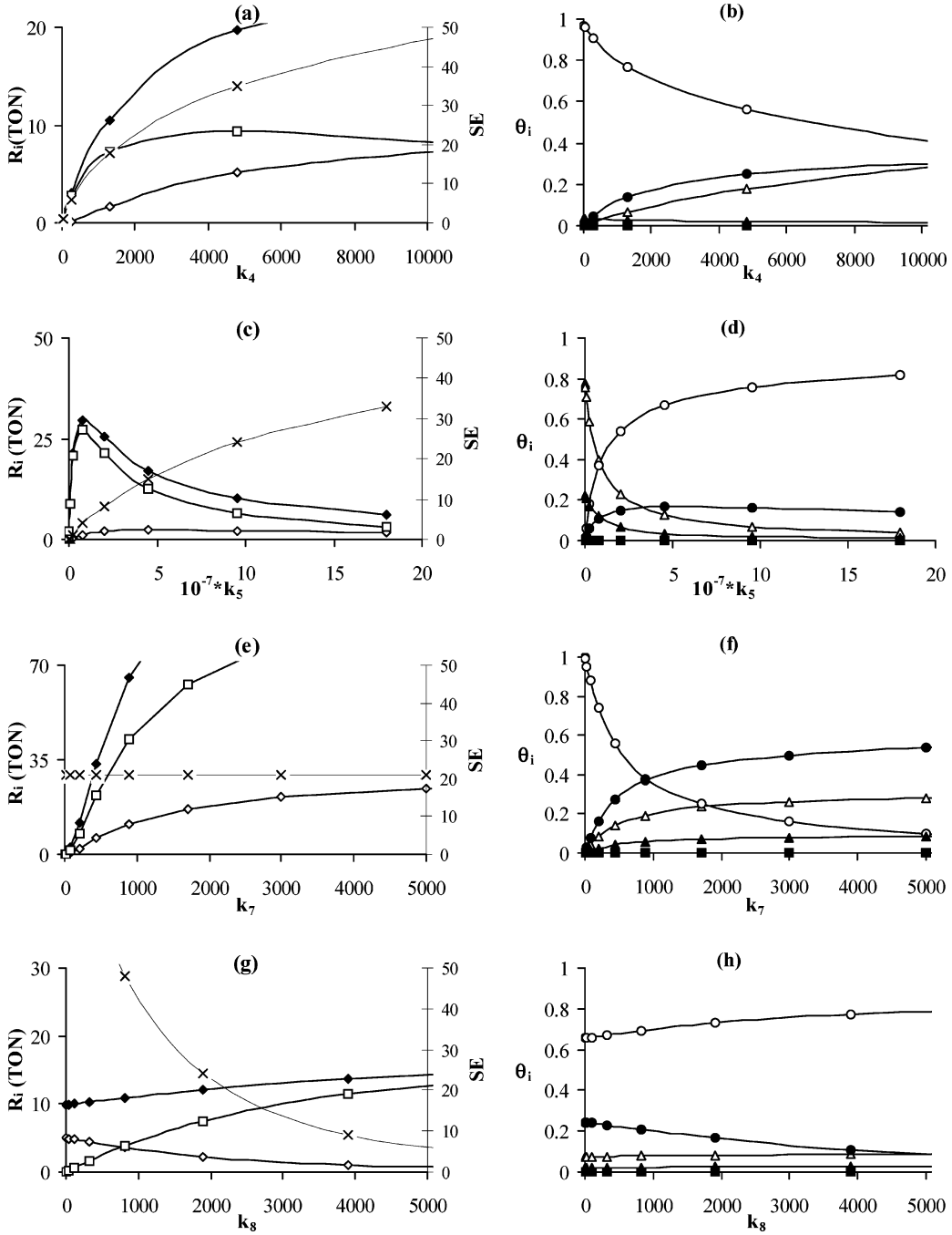

Figure 3. Production, R_i, and superficial coverage, θ_i, for the changes in the various kinetics parameters, k_i, of the mechanism of Scheme 1 at 533 K and $p_{CO} = 20.52$ and $p_{NO} = 39.59$ Torr. The lines have been drawn to guide the eyes. (◆) R_{CO_2}; (◇) R_{N_2}; (□) R_{N_2O}; (X) SE; (Δ) θ_{CO}; (▲) θ_{NO}; (●) θ_N; (○) θ_O; (■) θ_V.

TABLE 2: Experimental and Theoretical Productions (MC and MFT) at Different Temperatures[a]

		R_{CO_2} (TON)			R_{N_2} (TON)			R_{N_2O} (TON)			
T (K)	EXP	MFT	MC (sqr)	MC (hex)	MFT	MC (sqr)	MC (hex)	MFT	MC (sqr)	MC (hex)	nn/(nn + nnd)
453	2.05	0.01	0.009	0.0097	0	0	0	0.01	0.009	0.008	
473	3.42	0.20	0.193	0.191	0	0.0026	0.002	0.19	0.186	0.192	0.3396
493	5.6	2.08	1.73	1.915	0.06	0.10	0.091	1.97	1.534	1.736	0.2912
513	9.19	7.52	0.393	1.842	0.61	0.071	0.34	6.30	0.30	1.17	0.03219
533	14.95	12.25	0	0.01	2.13	0	0.007	7.99	0	0.002	0

[a] Square lattice (sqr); hexagonal lattice (hex); $P_{CO} = 20.52$ Torr; $P_{NO} = 39.52$ Torr.

possible to obtain a better quantitative description from the experimental observations given the approximations of the model, which do not include aspects such as the dependence of the activation energies and the sticking factors on surface coverage and temperature. In the experiment, the Pd particles also show the phenomenon of surface heterogeneity, which the mean field theoretical model does not consider by assuming a single type of adsorption sites.

The fitting parameters that we have obtained, which are included in Table 1, represent a set of reasonable parameters

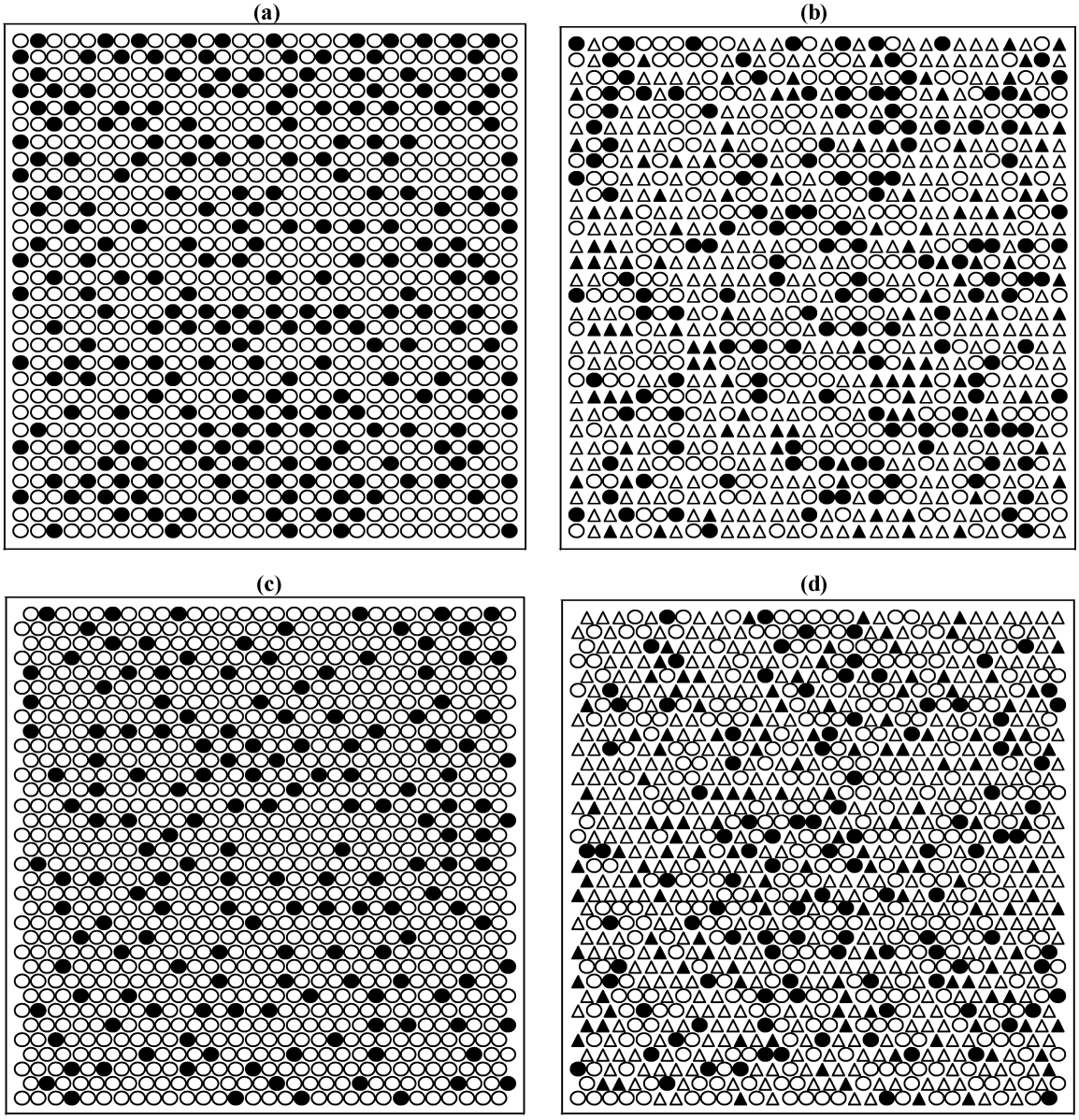

Figure 4. Snapshots of the MC simulations in the steady state for the reactive and poisoned surface and the constants of Table 1; $p_{CO} = 20.52$ and $p_{NO} = 39.52$ Torr. (a) Square lattice and uniform surface for $T = 533$ K. (b) The same as (a) for $T = 493$ K. (c) Hexagonal lattice and uniform surface for $T = 533$ K. (d) The same as (c) for $T = 493$ K. (△) CO; (▲) NO; (○) O; (●) N; (■) vacuum.

for the CO−NO reaction on Pd at moderate pressures, and they can be the basis for analyzing some general characteristics of the system. Figure 2a, for example, shows the behavior of productions with temperature, calculated from the analytical equations and the fitting parameters at the experimental pressures. The inset of the figure shows the selectivity of nitrogen, defined by equation A-13.

In the first place, the maximum of the production curves with temperature stands out, and that has been found experimentally by G. Prevot et al.[6] for UHV, by K. Nakao et al.[7] in the low-pressure zone, and by K. Thirunavukkarasu et al.[8] for various proportions of the reactants. The selectivity curve, on the other hand, increases with temperature and shows an interval, outside which only one of the products that contains nitrogen is produced. In the case of the pressures used in this work, for example, production of only N_2O is observed below approximately 450 K and that of only N_2 above 700 K.

The maximum of the production curves has, as a consequence, an interesting change of sign in the order seen for the reactants in the overall reaction, showing a change in behavior of the system between the low- and high-temperature zones. This is shown in Figure 2b and d for order m with respect to CO and in Figure 2c and e for order n with respect to NO, defined by the expression

$$R_i = k_i \, p_{CO}{}^m p_{NO}{}^n \tag{4}$$

The analytical solution of the kinetic model detailed in Appendix A shows the sensitivity of production and the surface coatings with respect to the modification of the parameters of the various elemental steps. Figure 3 illustrates the variations of the kinetics of some of the fitting parameters at 533 K, $p_{CO} = 20.52$ Torr, and $p_{NO} = 39.5$ Torr. In every case in the figures, one of the parameters has been varied while keeping the others constant.

Table 2 summarizes the information on production versus temperature according to various techniques used in this work, laboratory experiments, mean field model calculation, and MC simulations over a square and a hexagonal lattice. First of all, the behavior of the CO−NO reaction over a square crystal lattice

for the set of fitting parameters, at the moderate pressures of the experiment and at temperatures higher than 500 °C, determined by Monte Carlo (MC) simulations, should be pointed out. This behavior is similar to that found by MC in the classical work of Yaldram and Khan,[21] Brosilow and Ziff,[22] and Meng, Weinberg, and Evans,[23] where the surface poisoning of a simplified mechanism of the CO−NO reaction over a square lattice was explained with the BZ checkerboard argument.[22,23] In this theoretical model, the superficial configuration was transformed into absorbent or poisoned because the nitrogen atoms achieved a configuration formed by poisoned sectors, each of which the nitrogen atoms occupied, for example, the white or black squares of a checkerboard. In a recent paper by our group,[24] we extended the argument to the case of the surface of a three-dimensional fractal.

We wish to point out that, in the system that is being studied, there is a situation similar to the previous one for high temperatures in the case of a square lattice, despite including the complete mechanism of Scheme 1, which considers even the desorption steps of CO and NO. In Table 2, the production determined in the MC simulation decreases strongly, in that case, with temperature, to the same extent that the fraction of pairs of next neighbor (nn) nitrogen atoms decreases until all of the superficial nitrogen atoms are configured as diagonal pairs (nnd) that are inert for reacting according to step 6. In the table, it is also seen that, in that case, the production determined from the simulations is different from that calculated from a MFT model such as that of the kinetics equations. This is understandable because the MFT model determines only mean values that do not take into account the information on the configuration of the adsorbed phase. The MFT model, on the other hand, coincides with the MC simulations over a square lattice when the fraction of nondiagonal nitrogen is sufficiently high, which occurs at temperatures below 500 K. In all of the simulations, however, the production is equal to the product of the corresponding kinetics constant and to the fraction of next neighbor pairs (nn). It is seen, therefore, that the effect of the surface heterogeneity is detected by the MC simulations and not by the MFT model.

With the purpose of going deeper into this aspect, MC simulations were made for the same temperatures over a hexagonal lattice, and the results are included in Table 2. Once again, the system becomes unreactive at high temperatures due to the configurational situation of the adsorbed phase. At lower temperatures, there is coincidence between the productions determined by MC on both kinds of lattices, they become different as the temperature increases, and complete poisoning occurs at high temperatures. A similar situation is seen in the phase diagrams that are not shown, which coincide, in all cases, at lower temperatures and become different at high temperatures.

Figure 4 shows some snapshots of the configurations of the superficial phase corresponding to the square and hexagonal lattices in a reactive and a poisoned situation. In the case of the square lattice and the reactive system, there is a substantial number of nn nitrogen atoms. When the surface is poisoned and the system is unreactive, there is a high percentage of nitrogen atoms in diagonal positions. In the case of the hexagonal lattice, on the other hand, there is only one type of pairs of nitrogen neighbors. In the case of poisoning, where the adsorbed phase consists only of nitrogen and oxygen atoms, it is caused by the isolation of the nitrogen atoms which remain on the surface surrounded by superficial atoms of oxygen.

The experimental results at high temperatures show a reactive system that can be interpreted, as is often done, by a mean field

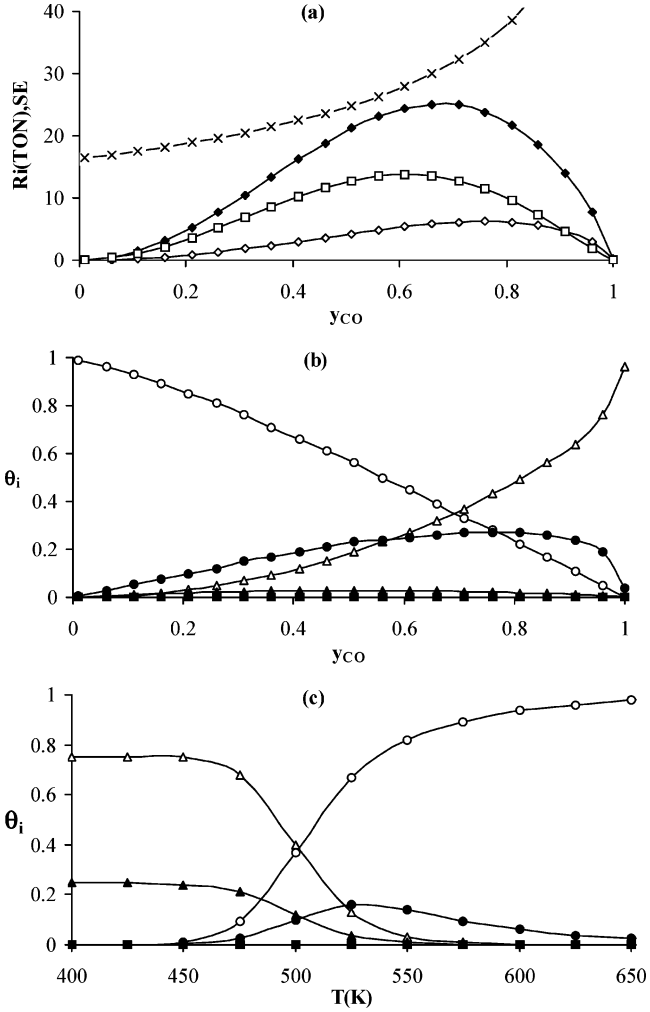

Figure 5. (a) Production (R_i,y_{CO}) at T = 533 K, (b) phase diagram (θ_i,y_{CO}) at T = 533 K, and (c) coverage versus temperature (θ_i,T) ($p_{CO} + p_{NO}$) = 60 Torr in the steady state for the constants of Table 1 and the MFT model.

model like that of the kinetics equations, which does not introduce the surface configuration in the calculations.

Figure 5a shows the production and selectivity curves versus CO concentration in the gas phase, and Figure 5b shows the phase diagram, corresponding to 533 K and a total pressure of the gas phase equal to 60 Torr, determined by MFT. The production curves show, in a manner similar to what was obtained in Figure 3 with temperature, a maximum with y_{CO}. This behavior has been seen experimentally in work reported recently.[6,8] The behavior of the phase diagram according to the mean field model shows a decrease of the oxygen obtained by dissociation of the NO adsorbed on the surface with increasing concentration of CO, whose later adsorption and reaction eliminates the superficial oxygen through eq 7, producing CO_2. The unreacted CO particles become an adsorbed phase that increases with y_{CO} until the surface is poisoned when, in the gas phase, there is no NO. The adsorbed nitrogen phase increases with y_{CO} from zero to a maximum of 27% at this temperature for y_{CO} = 0.8, dropping to zero at the end of the diagram. In the whole concentration range, there is a very small fraction of adsorbed NO particles and vacant sites.

Figure 5c shows the variation of the surface coverage with temperature at the pressures p_{CO} = 20.52 and p_{NO} = 39.52 Torr of the experiments, which correspond to y_{CO} = 0.34. It is seen that the surface is covered with CO and NO at low temperatures,

and it is poisoned with oxygen, which starts appearing at 450 °C, and a small percentage of nitrogen, at high temperatures.

Conclusions

Considering a mechanism similar to that used by Peden and Permana for the CO−NO reaction on Rh, a set of kinetics parameters have been determined that interpret experiments for the production of CO_2 and the selectivity for nitrogen versus temperature for the same reaction on Pd.

It is seen that at temperatures higher than 530 °C, the system described by the conditions of the previous point simulated by the Monte Carlo method on a square lattice shows a behavior similar to that of the classical model described by Brosilow and Ziff with a poisoned surface due to a superficial configuration in which the nitrogen atoms occupy the "white or black squares" of a checkerboard. In the case of a hexagonal lattice, the same poisoning is seen, but in this case, it is due to a configuration with isolated nitrogen atoms on the surface surrounded by atoms of adsorbed oxygen.

The production versus temperature and the production versus CO concentration in the gas-phase curves show a maximum according to the experimental reports in the literature.

A change in the sign of reaction order with respect to CO and NO between the high- and low-temperature zones is seen in Figure 2.

Selectivity for nitrogen shows a rising curve with temperature.

Appendix A

Analytical Solution of the Reaction Model Used in the Paper. In a manner similar to the development shown in one of our previous papers,[25] we will synthesize the equations used in this paper for the mechanism of Scheme 1. Since it is assumed that the $CO_{(a)}$ and $NO_{(a)}$ adsorbates are in equilibrium with the gas phase, it is possible to write the relations

$$K_{CO} = \frac{\theta_{CO}}{\theta_S P_{CO}} \quad K_{NO} = \frac{\theta_{NO}}{\theta_S P_{NO}} \tag{A1}$$

where the equilibrium constants are expressed as functions of the coverages θ_{CO} and θ_{NO} and the partial pressures P_{CO} and P_{NO} of the gas phase, and θ_S represents the coverage of the vacant surface sites. The procedure used consists of expressing the coverages θ_i as functions of θ_{CO}, for which, if we define

$$A = \frac{P_{NO}K_{NO}}{P_{CO}K_{CO}} \tag{A2}$$

$$B = \frac{1}{P_{CO}K_{CO}} \tag{A3}$$

it is possible to write the relations

$$\theta_{NO} = A\theta_{CO} \quad \theta_S = B\theta_{CO} \tag{A4}$$

The following conservation equations can be written, where the first two represent the steady state for the surface species $N_{(a)}$ and $O_{(a)}$ ($d\theta_N/dt = 0$ and $d\theta_O/dt = 0$)

$$k_5\theta_{NO}\theta_S - 2k_6\theta_N^2 - k_8\theta_{NO}\theta_N = 0 \tag{A5}$$

$$k_5\theta_{NO}\theta_S - k_7\theta_{CO}\theta_O = 0 \tag{A6}$$

$$\theta_S + \theta_{CO} + \theta_{NO} + \theta_N + \theta_O = 1 \tag{A7}$$

If we define the relations

$$C = (-k_8A + ((k_8A)^2 + 8k_5k_6AB)^{1/2})/4k_6 \tag{A8}$$

$$D = k_5AB/k_7 \tag{A9}$$

it is possible to write

$$\theta_N = C\theta_{CO} \quad \theta_O = D\theta_{CO} \tag{A10}$$

so that from A7, we have

$$\theta_{CO} = 1/(1 + A + B + C + D) \tag{A11}$$

Therefore, the productions R_i are the following

$$R_{CO_2} = k_7\theta_{CO}\theta_O \quad R_{N_2} = k_6\theta_N^2 \quad R_{N_2O} = k_8\theta_{NO}\theta_N \tag{A12}$$

and the selectivity SE for the nitrogen is defined by

$$SE = R_{N_2}/(R_{N_2} + R_{N_2O}) \tag{A-13}$$

Appendix B

Simulation Procedure. The MC algorithm used in this paper is similar to one used previously by our group[26] for the CO oxidation reaction, based on one proposed earlier for this system[27] and recently for the CO−NO reaction.[28] For the CO−NO reaction, the simulation process starts by selecting an event from the mechanism (adsorption, desorption, dissociation, or reaction) according to the probability, p_i, of the event defined by

$$p_i = k_i/\sum_i k_i \tag{B1}$$

where k_i corresponds to the rate constant of step i of the mechanism. It is assumed that the rate constants k_i can be expressed as functions of temperature T according to Arrhenius's equation

$$k_i = \nu_i \exp(-E_i/RT) \tag{B2}$$

where E_i is the activation energy and ν_i is the frequency factor. In the case of adsorption, k_i is calculated according to the expression of the kinetic theory of gases

$$k_i(\text{ads}) = S_i\sigma(2\pi M_i RT)^{-1/2} \tag{B3}$$

where M_i is the molecular mass of i, S_i is the corresponding sticking coefficient, and the coefficient σ is the area occupied by 1 mol of superficial metal atoms.

The MC algorithm begins with selection of the event. If it corresponds to the adsorption of CO, a site is chosen randomly on the surface, and if it is vacant, a $CO_{(a)}$ particle will be adsorbed. If the site is occupied, the attempt is ended. If the adsorption of NO is chosen, the procedure is completely analogous, and a $NO_{(a)}$ particle is adsorbed.

If CO desorption is chosen, a surface site is selected randomly. If it is occupied by a particle different from $CO_{(a)}$ or if it is vacant, the attempt is ended. However, if it is occupied by a $CO_{(a)}$ particle, desorption occurs, and the particle is replaced by a vacant site. The procedure is analogous to the case of choosing the desorption of NO.

When the chosen event is the dissociation of NO, a surface site is chosen randomly. If it is occupied by a $NO_{(a)}$ particle, a nearest neighbor (nn) site is chosen randomly next to the first site. If this is empty, dissociation occurs, and a $N_{(a)}$ particle remains in the first site and an $O_{(a)}$ particle in the second site.

In the case of chemical reaction events that involve two reactant particles, a site on the surface is first chosen randomly. If it is occupied by a particle corresponding to one of the reactants, a nn site is then chosen randomly next to the first site. If the latter is occupied by the other particle of the same reaction, the event is successful, and a product molecule is removed from the surface, leaving two vacant sites. For example, if the first particle is $CO_{(a)}$ and the second is $O_{(a)}$, a molecule of CO_2 leaves the surface.

The substrates used in the simulations were a uniform surface made of sites located in an $L \times L$ square lattice, a hexagonal lattice, and a statistical fractal, the incipient percolation cluster (IPC), whose active sites were generated by blocking a fraction equal to 0.407254 of the $L \times L$ sites (impurities) of the square lattice, with a fractal dimension equal to 91/48.[29] The substrates were obtained, in this case, by considering only the spanning cluster of the remaining sites computed by Kopelman's algorithm.[30] Since the IPC is probabilistic or nondeterministic, it was necessary to generate a number of them so that the properties obtained from MC for the CO−NO reaction were the average of the results of the simulations carried out on those substrates.

In general, to reach an adequate stability in the results, use was made of a number of iterations of the order of 3×10^7 MCS (Monte Carlo steps), defined as a number of attempts equal to the number of sites in the substrate.

Acknowledgment. The authors thank FONDECYT N°1030759 and FONDAP N°11980002 for financial support of this work.

References and Notes

(1) (a) Taylor, K. C. *Catal. Rev. Sci. Eng.* **1993**, *457*, 35. (b) Shelef, M.; Graham, G. *Catal Rev. Sci. Eng.* **1994**, *36*, 433.

(2) (a) Nicolis, G.; Prigogine, I. *Self-Organization in Nonequilibrium Systems*; Wiley-Interscience: New York, 1977. (b) Haken, H. *Synergetics*; Springer-Verlag: New York, 1977. (c) Marro, J.; Dickman, R. *Nonequilibrium Phase Transitons in Lattice Models*; University Press: Cambridge, U.K., 1999.

(3) Evans, J. W. *Langmuir* **1991**, *7*, 2514.

(4) Zhadanov, V. P.; Kasemo, B. *Surf. Sci. Rep.* **1994**, *20*, 111.

(5) (a) Albano, E. V. *Heterog. Chem. Rev.* **1996**, *3*, 389. (b) Albano, E. V.; Borowko, M. *Computational Methods in Surface and Colloid Science*; Marcel Dekker: New York, 2000; Chapter 8, pp 387−437.

(6) Prévot, G.; Henry, C. *J. Phys. Chem. B* **2002**, *106*, 12191.

(7) Nakao, K.; Ito, S.; Tomishige, K.; Kunimori, K. *J. Phys. Chem. B* **2005**, *109*, 17579.

(8) Thirunavukkarasu, K.; Thirumoorthy, K.; Libuda, J.; Gopinath, Ch. *J. Phys. Chem. B* **2005**, *109*, 13272.

(9) Rainer, D. R.; Vesecky, S. M.; Koranne, M.; Oh, W. S.; Goodman, D. W. *J. Catal.* **1997**, *167*, 234.

(10) Rainer, D. R.; Koranne, M.; Vesecky, S. M.; Goodman, D. W. *J. Phys. Chem. B* **1997**, *101*, 10769.

(11) Hecker, W. C.; Bell, A. T. *J. Catal.* **1983**, *84*, 200.

(12) (a) Oh, S. H.; Fisher, G. B.; Carpenter, J. E.; Wayne, D. *J. Catal.* **1986**, *100*, 360. (b) Oh, S. H.; Eickel, C. C. *J. Catal.* **1991**, *128*, 526.

(13) (a) Cho, B. K. *J. Catal*. **1992**, *138*, 255. (b) Cho, B. K. *J. Catal*. **1994**, *148*, 697.

(14) Chuang S.; Tan, C. *J. Catal.* **1998**, *173*, 95.

(15) Peden, C.; Belton, D.; Schmieg, S. J. *J. Catal*. **1995**, *155*, 204.

(16) (a) Permana, H.; Simon, K.; Peden, C.; Schmieg, S. J.; Belton, D. *J. Phys. Chem.* **1995**, *99*, 16344. (b) Permana, H.; Simon, K.; Peden, C.; Schmieg, S. J.; Lambert, D. K.; Belton, D. *J. Catal.* **1996**, *164*, 194.

(17) Cortés, J.; Valencia, E. *J. Phys. Chem. B* **2004**, *108*, 2979.

(18) Cortés, J.; Valencia, E. *J. Phys. Chem. B* **2006**, *110*, 7887.

(19) (a) Zaera, F.; Gopinath, Ch. S. *J. Chem. Phys.* **1999**, *111*, 8088. (b) Zaera, F.; Gopinath, Ch. S. *Chem. Phys. Lett.* **2000**, *332*, 209. (c) Zaera, F.; Gopinath, Ch. S. *J. Chem. Phys.* **2002**, *116*, 1128.

(20) (a) Cortés, J.; Puschmann, H.; Valencia, E. *J. Chem. Phys.* **1996**, *105*, 6026. (b) Cortés, J.; Puschmann, H.; Valencia, E. *J. Chem. Phys.* **1998**, *109*, 6086. (c) Dickman, A.; Grandi, B. C.; Figueiredo, W.; Dickman, R. *Phys. Rev. E* **1999**, *59*, 6361. (d) Valencia, E.; Cortés, J. *Surf. Sci.* **2000**, *470*, L109. (e) Cortés, J.; Valencia, E. *Physica A* **2002**, *309*, 26. (f) Cortés, J.; Valencia, E. *J. Phys. Chem. B* **2004**, *108*, 2979.

(21) Yaldram, K.; Khan, M. A. *J. Catal.* **1991**, *131*, 369.

(22) Brosilow, B. J.; Ziff, R. M. *J. Catal.* **1992**, *136*, 275.

(23) Meng, B.; Wienberg, W. H.; Evans, J. W. *Phys. Rev. E* **1993**, *48*, 3577.

(24) Cortés, J.; Valencia, E. *Phys. Rev. E* **2004**, *68*, 16111.

(25) Cortés, J.; Araya, P.; Betancourt, F.; Díaz, F. *J. Chem. Res.* **2004**, *1*, 68.

(26) Cortés, J.; Valencia, E.; Araya, P. *J. Chem. Phys.* **1998**, *109*, 5607.

(27) (a) Araya, P.; Porod, W.; Wolf, E. E. *Surf. Sci.* **1990**, *230*, 245. (b) Araya, P.; Porod, W.; Snat, R.; Wolf, E. E. *Surf. Sci.* **1989**, *180*, 208.

(28) Olsson, L.; Zhdanov, V. P.; Kasemo, B. *Surf. Sci.* **2003**, *529*, 338.

(29) Stauffer, D.; Aharony, A. *Introduction to Percolation Theory*, 2nd ed.; Taylor and Francia: London, 1992.

(30) (a) Hoshen, J.; Kopelman, R. *Phys. Rev. B* **1976**, *14*, 3438. (b) Kopelman, R. *J. Stat. Phys.* **1986**, *42*, 185.